Mechanistic Insights into the Palladium-Catalyzed Aziridination of Aliphatic Amines by C–H Activation

Adam P. Smalley, Matthew J. Gaunt*

Department of Chemistry, University of Cambridge, Lensfield Road, Cambridge CB2 1EW, United Kingdom

ABSTRACT: Detailed kinetic studies and computational investigations have been performed to elucidate the mechanism of a palladium-catalyzed C–H activation aziridination. A theoretical rate law has been derived which matches with experimental observations and has led to an improvement in the reaction conditions. Acetic acid was found to be beneficial in controlling the formation of an off-cycle intermediate, allowing a decrease in catalyst loading and improved yields. Density functional theory (DFT) studies were performed to examine the selectivities observed in the reaction. Evidence for electronic-controlled regioselectivity for the cyclopalladation step was obtained by a distortion-interaction analysis while the aziridination product was justified through dissociation of acetic acid from the palladium(IV) intermediate preceding the product-forming reductive elimination step. The understanding of this reaction mechanism under the synthetic conditions should provide valuable assistance in the comprehension and design of palladium-catalyzed reactions on similar systems.

Introduction

Transition metal catalyzed activation of aliphatic C–H bonds has emerged as an area of great potential for chemical synthesis through the development of new transformations, the streamlining of complex molecule assembly and in the late-stage modification of biologically important entities.[1] Central to the activation of many of these traditionally unreactive C–H bonds is a process called cyclometallation, a functionalization event that steers the metal catalyst to the point of reaction and drives the C–H bond cleavage through proximity; coordination of the metal catalyst to a Lewis basic heteroatom within the directing motif is assumed to lower the entropic and enthalpic costs of the C–H bond cleavage and ring closure.[2] Reaction of the resulting metallocycle with an external species, to form a carbon-carbon or carbon heteroatom bond, completes the overall functionalization process. Several functionalities can participate in this 'directed' C–H activation, such as carbonyl derivatives, aromatic nitrogen heterocycles and hydroxyl motifs,[3] and, arguably, palladium complexes have been most successful at promoting catalytic C–H functionalization in aliphatic systems. As a result, cyclopalladation has underpinned a number of useful catalytic aliphatic C–H bond functionalization processes that have expanded the toolbox of reactions available to synthetic chemists.

Given the palladium-coordinating ability of aliphatic amines, it is surprising that they are seldom used in catalytic C–H activation reactions in comparison to other, synthetically important and polar functional groups.[4] However, it is precisely this strong coordination that limits their utility in C–H activation. When treated with palladium(II) salts, two molecules of the aliphatic amine coordinate to the electrophilic metal center to form coordinately saturated square-planar complexes, a species which is often unreactive to C–H cleavage (Figure 1(a)).[5] As a result, C–H activation on aliphatic amines requires their derivatization with electron-withdrawing protecting groups or bespoke directing groups in order to achieve a successful reaction, which reduces the overall efficiency of the C–H transformation. Aliphatic amines are, however, particularly important functional groups as they are common in pharmaceuticals, synthetic building blocks, natural products and polymeric materials. Therefore, the development of new catalytic C–H activation modes for aliphatic amines is an important challenge for the continual advance of chemical synthesis.

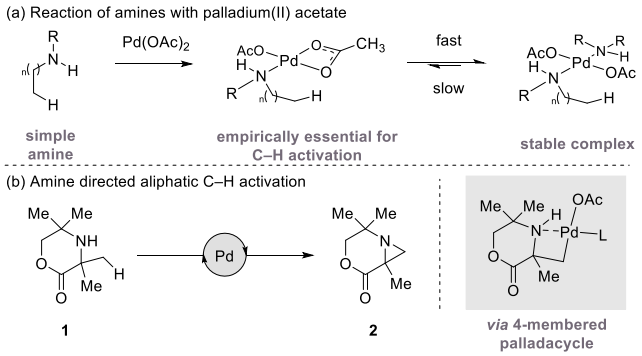

Figure 1. (a) Amine coordination to palladium(II) salts results in stable complex formation; (b) The system under study in this report – amine directed aliphatic C–H functionalization.[6]

As part of our overarching goal to develop new activation modes for catalytic C–H activation, our group recently reported the use of an unprotected aliphatic secondary amine to direct a palladium-catalysed C–H functionaliza-

tion (Figure 1(b)). This activation mode resulted in the transformation of a methyl group adjacent to the amine motif *via* a four-membered ring cyclopalladation pathway.[6] In one of the two novel transformations detailed in that initial report, we described a C–H amination to form aziridines. A fully substituted and unsymmetrical secondary amine, morpholinone **1**, underwent C–H activation to form a four-membered ring palladacycle which, following the action of a hypervalent iodine oxidant, promoted C–N bond formation to aziridine **2**. This aziridination had several interesting features which would have been difficult to predict with the current understanding of C–H activation processes.

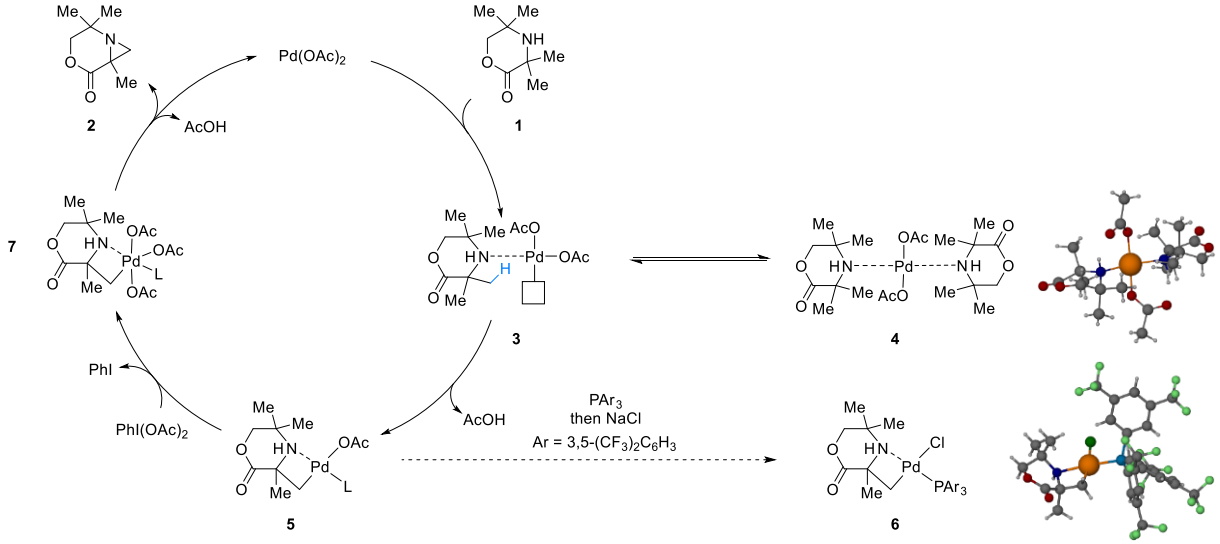

Figure 2. Postulated mechanism based on our previous study[6] along with intermediates characterized by X-ray crystallography. The morpholinone **1** coordinates to the metal catalyst, but can only undergo C–H activation when there is a vacant coordination site. The palladacycle **5** is presumably oxidized to a palladium(IV) species **7** ('L' is an undefined neutral ligand) which can then reductively eliminate to give the product **2**. The palladacycle **5** was observed through crystallization on addition of a phosphine ligand to give **6**.

While a comprehensive understanding of this reaction mechanism would allow us to logically move towards further reaction optimization, we also wanted to rationalize (a) why the cyclopalladation occurred with extremely high regioselectivity, even though there appeared to be a choice of sites to react and (b) why an aziridine was furnished as the final product, unlike the acetoxylated product often obtained under similar conditions.[3a, 7]

Herein we report detailed mechanistic studies on the palladium-catalyzed aziridination of tetramethylmorpholinone **1**. Furthermore, density functional theory (DFT) calculations were performed to gain additional insight into the reaction. As a result, we were able to gain a comprehensive understanding of the factors that influence the catalytic C–H activation reaction and improvements in the reaction conditions for aziridination were realized.

Results and Discussion

At the outset of our studies, we were able to propose a basic reaction mechanism upon which we could formulate more advanced studies (Figure 2). We had previously observed that mixing two equivalents of the amine **1** with palladium acetate resulted in the isolable *bis*-amine palladium(II) complex **4**. On warming this complex, we had been able to identify a putative C–H activation complex **5**, which, following treatment with a phosphine, resulted in the mono-nuclear cyclopalladation species **6**, as determined by X-ray diffraction of a single crystal. The catalytic cycle was believed to conclude with oxidation of the palladacycle by the hypervalent iodine $PhI(OAc)_2$ followed by C–N reductive elimination of the resulting palladium(IV) species **7**.

Kinetic Studies

Our kinetic protocol features experiments to probe the reagent concentration dependencies and isotopic labelling to interrogate the mechanism of the reaction in Figure 2. The process was monitored by aliquotting the reaction mixture and measuring the concentration by gas chromatography (GC) with 1,1,2,2-tetrachloroethane as an internal standard. The original reaction conditions involved the treatment of amine **1** with 5 mol% palladium acetate, 1.5 equivalents of $PhI(OAc)_2$, 2.0 equivalents of acetic anhydride in a solution of toluene stirred at 70 °C. However, in order to simplify the system and remove any extraneous factors that may complicate the analysis we monitored the reaction with just starting amine, catalyst,

oxidant and solvent. This led to a rate profile that appeared to be linear, but was only ~30% complete in 500 minutes (see Supporting Information). Doubling the concentration of catalyst to 10 mol% allowed us to follow the whole reaction over an appreciable timescale and revealed that the reaction rate *increases* during the majority of the reaction (up to ~90% conversion) and only levels off at the very end (Figure 3). Notably, the rate of product formation is roughly equal to the rate of starting material usage and so our analyses using initial rates are based on starting material concentration so as to minimize any errors in the concentration measurement.

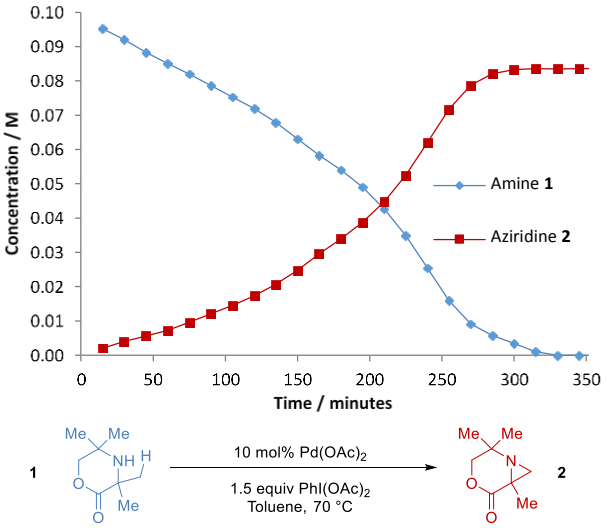

Figure 3. Reaction profile for the above aziridination.

The increase in reaction rate over time suggested to us that there was either a negative order dependence on amine **1**[8] or that the reaction was autoinductive. The autoinduction could be a result of rate acceleration by the action of product aziridine **2**, or by the acetic acid or phenyl iodide by-products. To test for autoinduction, same 'excess' experiments were performed.[9] This analysis is equivalent to carrying out identical reactions at two different starting points and is often used to probe product inhibition and catalysis deactivation. In this case, the reaction was started at 20% completion. If a (by-)product catalyzes the reaction, the reaction starting at 20% completion will be slower than the reaction that started from 0% completion. Simply overlaying the plots, after adjusting the 20% completion reaction for time so that the initial amine concentrations are equivalent, shows that there are negligible differences in the rate profiles (Figure 4). We also tested the effect of adding the (by-)products (0.2 equiv PhI, 0.2 equiv aziridine **2** or 0.4 equiv AcOH) to the 20% completion reaction. In the cases of PhI and aziridine **2** negligible differences in the rate was observed. However, if we added 0.4 equiv AcOH to the reaction then a marginal increase in rate was observed (see Supporting Information). While these results suggested that the result was not autoinductive, we did note the effect of AcOH and this is discussed in more detail later.

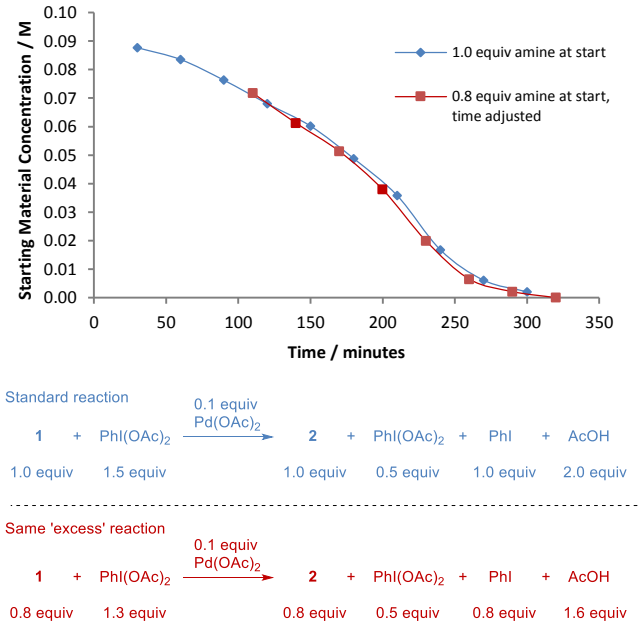

Figure 4. Probing potential autoinduction by carrying out two reactions at the same 'excess' but different initial amine concentrations.[9] The two plots overlay when time adjusted suggesting that there is no autoinduction. Reaction conditions for 1.0 equiv amine: amine **1** (0.10 M), $Pd(OAc)_2$ (0.01 M), $PhI(OAc)_2$ (0.15 M), toluene, 70 °C.

Therefore, we reasoned that the rate increase was due to a negative order dependency of amine **1**. By comparing the initial rate of reaction with that at 50% conversion, we saw that the rate had doubled, suggesting an approximate order of -1 with respect to substrate. However, as the rate decreases at the end, the situation is more complex than this (*vide infra*).

The order with respect to reaction of the other components in the mixture was then investigated. Due to the linear nature of the kinetic profile at the start of the reaction, the initial rate may be determined from the gradient of the concentration profile during this period. It was found that the reaction is zero-order with respect to $PhI(OAc)_2$, suggesting that the turn-over limiting step (TOLS) occurs before the oxidation step. Furthermore, the linear variation of rate with catalyst concentration revealed that the reaction was first order with respect to $Pd(OAc)_2$ (see Supporting Information).

Further kinetic information was obtained by measurement of the kinetic isotope effect (KIE). To prevent any possible regioselectivity issues between the two sets of methyl groups on amine **1** that may interfere with labeling experiments, we opted to test a cyclohexane-derivative **8** on the basis that competing methylene C–H activation would be negligible.[10] After confirming that this substrate was viable in the C–H aziridination, the KIE was determined from initial rate measurements of substrates **8** and d_6-**8** (Scheme 1). A value of 3.8 was obtained which is indicative of a primary isotope effect, suggesting that C–H bond cleavage occurs as part of the TOLS.[11]

Scheme 1. KIE measured from comparison of initial rates of amines 8 and d_6-8.

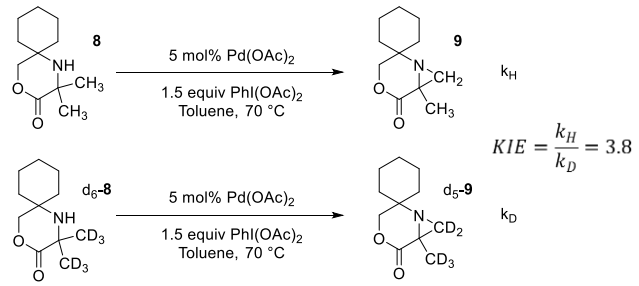

Consolidation of the mechanism proposed in Figure 2 with the above kinetic data allowed us to provide a set of kinetically-important elementary steps with which to test the experimental data (Scheme 2). An equilibrium exists whereby the amine **1** can coordinate to the catalyst to give mono-coordinated intermediate **10**. This intermediate can then undergo cyclopalladation in the TOLS or coordination with a second molecule of amine **1** to give the *bis*-amine complex **4**. It is proposed that the *bis*-amine complex **4** is an off-cycle intermediate and previous literature suggests that a vacant coordination site is required for C–H activation to occur *via* the assumed concerted metallation deprotonation pathway.[12] We assumed that any isomerization of the acetate ligands to provide the vacant site cis to the amine is expected to be so fast as to be kinetically negligible.[5]

Scheme 2. Proposed elementary steps in the kinetically important region of the catalytic cycle.

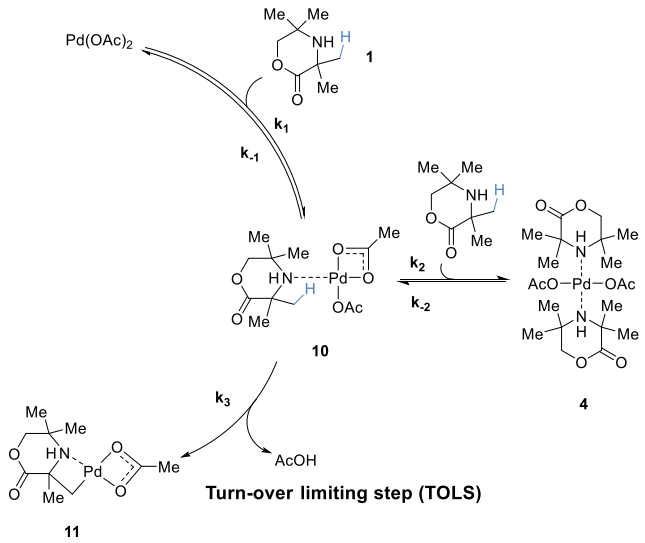

Evidence in support of this *bis*-amine complex being an off-cycle intermediate was obtained by comparing the reaction profiles of two sterically different amines. It was found that the aziridination of a more hindered amine **12** was faster than that of the tetramethyl amine **1** (Figure 5(a)). This could be indicative of faster C–H cleavage or an increased concentration of the active *mono*-coordinated species through destabilization of the off-cycle *bis*-amine complex on the basis of increased steric interactions between the amine and palladium center. In order to show that the rate increase was as a result of suppressing the formation of this unproductive species, a 1:1 mixture of the amines **1** and **12** was subjected to the catalytic conditions. Both species reacted at the same rate to form the corresponding aziridines **2** and **13** (Figure 5(b)). Notably, the rate of formation of **2** in the competition experiment is greater than observed in isolation. This suggests that the increased rate of reaction for the more hindered substrate (**12**) was not as a result of a lower energy C–H activation, but instead by alteration of the *mono*-/*bis*-amine equilibrium.

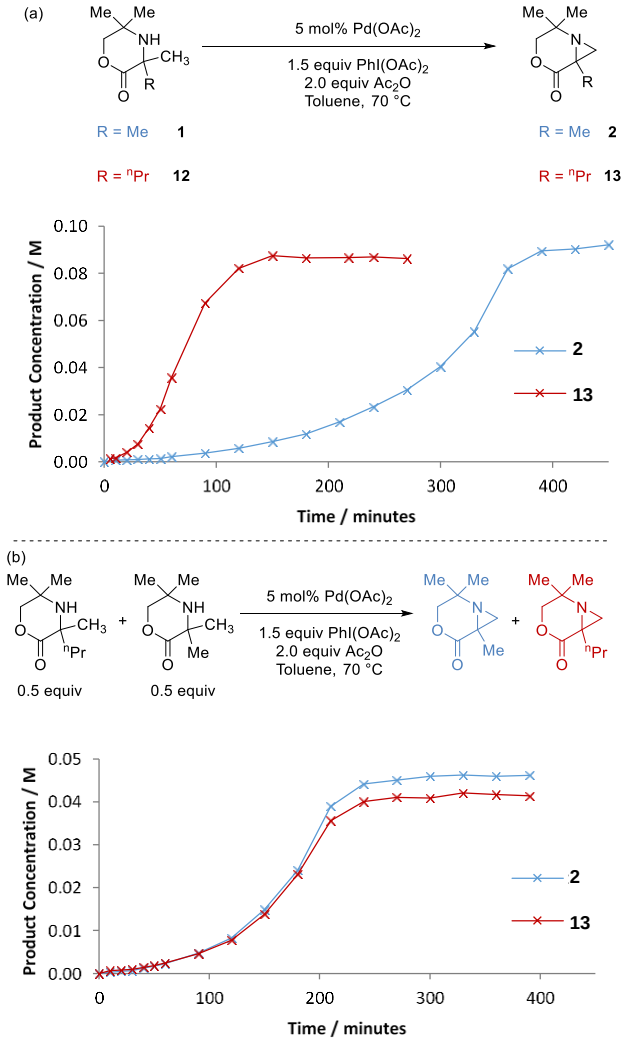

Figure 5. (a) The reaction rate of the more hindered amine **12** is faster than the tetramethyl amine **1**; (b) If these amines are mixed in a 1:1 ratio they both react at the same rate.

Next we set up a mathematical description of the reaction in order to allow quantitative agreement of our experimental data and qualitative insights. Because of the observed primary KIE, the rate of reaction is proposed to be given by the C–H activation step itself; this is also consistent with the measurement of oxidant concentration being zero order. To enable the derivation of the rate law, we assumed that all the intermediates following the TOLS provided a negligible contribution to the total catalyst mass. Consideration of the elementary steps in the reaction then led to the theoretical rate law (Scheme 3). This rate law accounts for the initial pseudo-1st order of reaction with respect to catalyst measured experimentally; initially the high substrate concentration can be considered a constant. The reaction is also negative 1st order with respect to substrate at high substrate concentrations, accounting for the increase in rate over the majority of the reaction, but changes to 1st order with respect to substrate at the end, accounting for the 'tailing-off' at the end of the reaction.

Scheme 3. Derivation of the Rate Law. Cat = $Pd(OAc)_2$ catalyst, $[Pd]_{total}$ = initial concentration of $Pd(OAc)_2$.

On-cycle

$$k_{-1}[\mathbf{10}] = k_1[\text{cat}][\mathbf{1}]$$

Off-cycle

$$k_2[\mathbf{10}][\mathbf{1}] = k_{-2}[\mathbf{4}]$$

Catalyst mass balance

$$[Pd]_{total} = [cat] + [\mathbf{10}] + [\mathbf{4}] = [\mathbf{10}]\left(\frac{k_{-1}}{k_1[\mathbf{1}]} + 1 + \frac{k_2[\mathbf{1}]}{k_{-2}}\right)$$

Rate law

$$Rate = -\frac{d[\mathbf{1}]}{dt} = \frac{d[\mathbf{11}]}{dt} = k_3[\mathbf{10}] = \frac{k_3[Pd]_{total}}{\left(\frac{k_{-1}}{k_1[\mathbf{1}]} + 1 + \frac{k_2[\mathbf{1}]}{k_{-2}}\right)}$$

By assuming that the amine concentration, [**1**], is large, we can take the rate law derived in Scheme 3 and obtain an approximation for the initial rate (eq. 1). This assumption is based on the concentration of *bis*-amine complex **4** dominating [**10**] and [cat]; this is supported by computational calculations which suggest that the formation of **4** from **10** is favored by 8.43 kcal mol^{-1} (see Supporting Information).

$$Initial\ rate \approx \frac{k_{-2}k_3}{k_2}\frac{[Pd]_{total}}{[\mathbf{1}]} \quad (1)$$

Varying the concentration of amine **1** whilst keeping the catalyst concentration constant allows the determination of $k_{-2}k_3/k_2$ to be 0.12 ± 0.02 M s^{-1} (see Supporting Information). Unfortunately, attempts to directly measure k_2/k_{-2} by ^{1}H NMR were unsuccessful due to the overlapping peaks of the metal species and therefore we were unable to determine a value for the rate constant of C–H activation, k_3.

Kinetics led Reaction Optimization

We had previously found that the addition of 0.4 equivalents of acetic acid to the reaction mixture had a small, but still noteworthy effect on the rate of reaction. Based on this, we questioned whether a much higher concentration of acid could lead to a further increase in the rate of reaction. The presence of acid in the reaction mixture should lead to some protonation of the amine and set up an equilibrium between the protonated and free-based amine.[13] If a proportion of the amine is protonated, then it is no longer able to coordinate to the metal and the effective concentration of free-amine is lowered. As the reaction progresses, the acid equilibrium shifts to provide more free-based amine and effectively delivers a slow release of substrate. By keeping the amine concentration low, less palladium is sequestered in the unproductive off-cycle *bis*-amine complex **4** leading to an increase in the overall rate of reaction. This is conceptually related to an organocatalytic reaction reported by Black-

mond where control of an off-cycle species lead to rate acceleration.[14]

Hence, increasing the concentration of acid was found to increase the rate of reaction, although at very high acid concentrations this increase in rate was offset by degradation of the final product (Figure 6). Other acids, such as benzoic acid and pivalic acid, were also found to give rate acceleration. However, as the optimum acid loading was found to be 20 equivalents, acetic acid was used as it is cheaper and, as a liquid, its use is more practical. It is important to note that we have not ruled out the possibility that the acetic acid is hydrogen bonding to the amine **1** rather than formally protonating the amine, however this still provides the desired decrease in free substrate concentration.

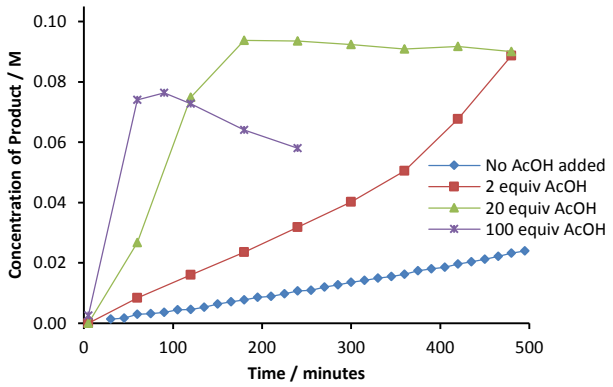

Figure 6. Increasing the concentration of acetic acid in the reaction mixture increases the rate of reaction. Reaction conditions: amine **1** (0.10 M), $Pd(OAc)_2$ (0.005 M), $PhI(OAc)_2$ (0.15 M), toluene, 70 °C.

Even though we believed that the beneficial addition of acetic acid was a result of limiting the formation of *bis*-amine intermediate **4**, it is important to consider other possible effects of acetic acid. Previous work by Ryabov[5] on an amine directed sp^2 C–H activation showed that addition of acid fully protonated the amine and changed the TOLS from C–H activation to dissociation of the $Pd(OAc)_2$ trimer. The subsequent C–H activation on this multi-metal complex was proposed to be faster due to the production of species with vacant coordination sites or more labile acetates. This explanation was unlikely here because even though $Pd(OAc)_2$ predominantly exists as a trimer in the solid phase and at 37 °C in benzene, it has been shown to exist as a monomer at 80 °C in benzene.[15] Nonetheless, this possibility was still ruled out by testing for a KIE with acetic acid present in the reaction. A primary KIE (of 3.9 vs 3.8 previously) was observed, indicating that the TOLS is still the C–H activation step. From the addition of acetic acid, we also noted that no H-incorporation was detected in the deuterated aziridine product, suggesting that the C–H/D activation step is not reversible under these conditions.

We also considered that a Fujiwara-type cationic intermediate may form,[16] whereby the C–H activation onto the putative cationic palladium species is faster, speeding up the reaction.[1(a),17] However, from initial observations this was judged to be unlikely as formation of the Fujiwara cationic species with acetic acid has only been reported with sp^2 C–H activations and trifluoroacetate ligands on palladium are required for sp^3 C–H activation *via* this method.[18] Addition of trifluoroacetic anhydride or trifluoroacetic acid was found to shut the reaction down while using palladium(II) trifluoroacetate instead of $Pd(OAc)_2$ as the catalyst led to a slower, poor yielding reaction.

We had previously noted[6] that acetic anhydride was beneficial to the reaction; however, unlike with acetic acid, changing the concentration of acetic anhydride had little effect. We suspect that the main effect of this additive is the removal of water.[19] Water was found to be detrimental to the reaction[20] and, furthermore, the removal of water by the anhydride leads to the production of rate accelerating acetic acid.

Taken together, addition of 20 equivalents of acetic acid and 2 equivalents of acetic anhydride led to an improved reaction, giving an isolated yield of 85% after 2.5 hours (Figure 7).

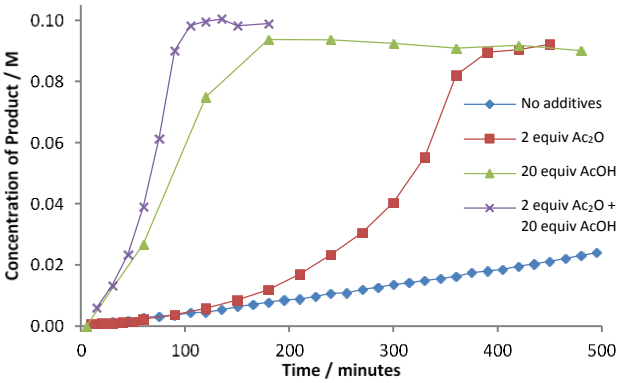

Figure 7. The effect of acetic acid and acetic anhydride additives on the reaction profile. Reaction conditions: amine **1** (0.10 M), $Pd(OAc)_2$ (0.005 M), $PhI(OAc)_2$ (0.15 M), toluene, 70 °C.

The generality of the newly optimized conditions were tested with a selection of amine substrates (Figure 8). Furthermore, the aziridination of amine **16** proceeded smoothly under the reaction conditions. This conversion of amine **16** to aziridine **17** rules out a general pathway for aziridination that proceeds first *via* acetoxylation and then displacement to form the 3-membered ring. It was found that the reaction worked well using industry-preferred ethyl acetate as the solvent.[21] The catalyst loading could also be lowered and reaction of amine **1** on a gram scale with 1 mol% $Pd(OAc)_2$ in ethyl acetate gave an 87% yield of the aziridine product.

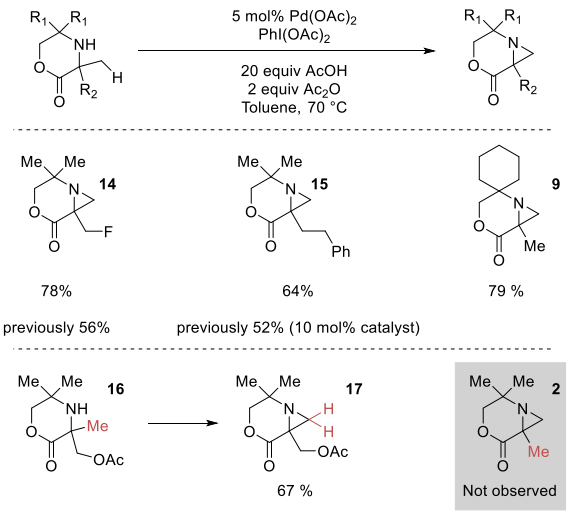

Figure 8. The optimized conditions have improved the yield of previous substrates.[6] In addition, amine **16** undergoes aziridination through C–H activation rather than S_N2-type displacement of acetate under the reaction conditions.

Computational Investigations

We next performed a series of density functional theory (DFT) studies to gain insights into the regioselectivity of the C–H activation step and the chemoselectivity of the C–N reductive elimination.[22] The calculations were performed using the Amsterdam Density Functional (ADF) program[23] at the relativistic ZORA-BLYP-D3/TZ2P level of theory, previously benchmarked for palladium catalysis with added dispersion corrections.[24] The inclusion of dispersion corrections has been shown to be important when bulky hydrocarbons are present as interactions which may previously have been considered as repulsive are, in fact, attractive.[25] Solvation by toluene was computed using the COSMO solvation model and vibrational frequency analysis was performed to confirm that the structures were either minima or transition states.

We first wanted to understand the regioselectivity of the C–H activation step. Initially, the geometry of the *mono*-coordinated intermediate **10** was calculated. It was found that there exists a hydrogen bond between one of the acetate ligands on the metal and the N–H of the substrate, similar to that seen in the crystal structure of the *bis*-amine complex **4** (Figure 2).[26] The other acetate ligand binds in a κ^2 mode so as to maximize bonding interactions. The transition states for C–H activation at the methyl groups either side of the nitrogen were then calculated. The cyclopalladation was proposed to occur *via* this *mono*-coordinated intermediate **10** from the above kinetic data and previous reports indicating the necessity of a vacant coordination site for C–H activation.[5,12(a)] The unlikelihood of an oxidative addition C–H activation, due to the resulting high energy palladium(IV) species which often require strong oxidants, and the large primary KIE suggesting a linear transition state,[10,27] meant that the mode of cyclopalladation was expected to proceed *via* a concerted metallation-deprotonation (CMD) pathway (Figure 9).[12b, 28]

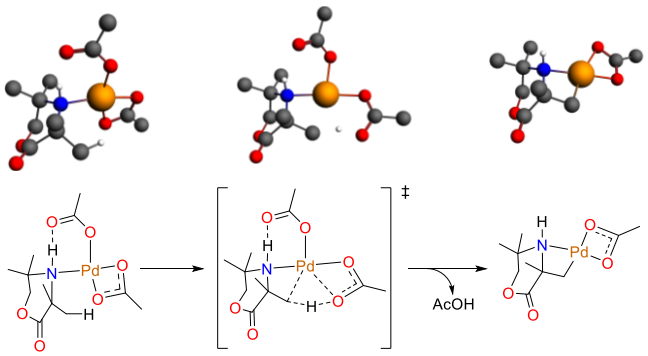

Figure 9. C–H activation through a concerted metallation-deprotonation pathway.

Application of this CMD approach on the two possible sites resulted in the transition state for the observed regioselectivity being lower in energy by 4.89 kcal mol^{-1} (Figure 10), suggesting that this mechanism is an appropriate representation of the cyclopalladation step.

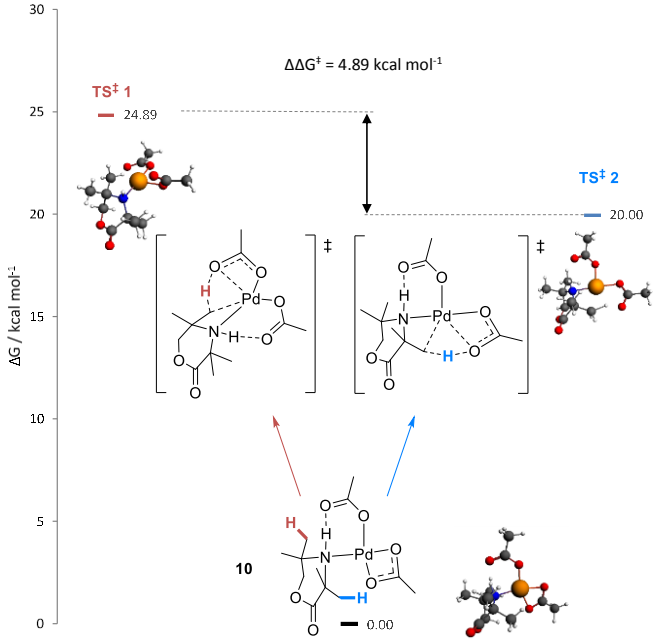

Figure 10. As expected from experiment, the transition state for C–H activation at the methyl groups nearest the carbonyl (**TS‡ 2**) is lower in energy than at the methyl groups furthest from the carbonyl (**TS‡ 1**).

We speculated that the observed selectivity was either a result of the difference in polarity of the methyl groups, due to differing distances from the carbonyl group, or from the change in shape of the ring caused by the ester motif. This question was probed using a distortion-interaction analysis, a method that has useful in understanding selectivity by splitting the activation energy into a steric and an electronic component.[29] Fragmentation of the transition state along the new bonds being formed and calculation of the interaction energy between these fragments in the transition state geometry allows us to

determine the distortion energy required to position the fragments in the required shape for reaction to occur. By fragmenting as shown in Figure 11 to reform the substrate and $Pd(OAc)_2$, we can see that the disfavored pathway actually has a lower distortion penalty (Table 1). This suggests that the flattening of the ring is not responsible for the selectivity. The increased distortion energy for the observed regioselectivity is offset by a greater increase in interaction energy, suggesting that it is the electronic effects of the carbonyl which are important. This can be explained by an increased acidity of the C–H bonds closest to the carbonyl in the ring, lowering the energy required to cleave the C–H bond during the metal activation step.[30] We believe that this analysis is valid, even though we fragment back past the *mono*-coordinated intermediate, as both pathways go through the exact same *mono*-coordinated intermediate **10**.

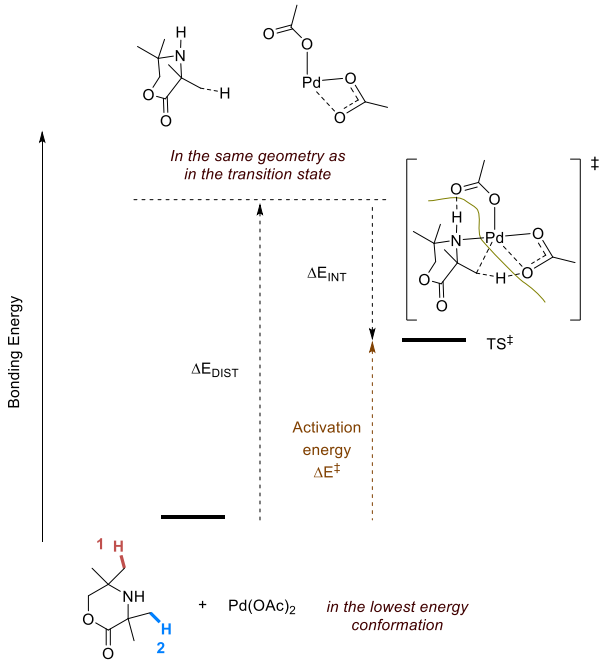

Figure 11. Distortion-interaction model splits the activation energy into two components. Fragmenting as shown in the TS‡ and calculating the interaction energy between the fragments gives the interaction energy (ΔE_{INT}). The distortion energy (ΔE_{DIST}) can subsequently be calculated from knowledge of the activation energy ($\Delta E^{‡}$).

Table 1. Distortion-interaction analysis of the two possible C–H activation pathways. Note that the small values for $\Delta E^{‡}$ are as a result of fragmenting back to the substrate and catalyst rather than the (lower energy) *mono*-coordinated intermediate (10)*

	$\Delta E^{‡}$	ΔE_{DIST}	ΔE_{INT}
TS‡ 1	2.70	85.12	-82.42
TS‡ 2	0.08	87.97	-87.89

*energies reported in kcal mol^{-1}

The reaction after the TOLS was proposed to proceed *via* oxidative addition of the palladacyle with $PhI(OAc)_2$ followed by C–N reductive elimination of the resulting palladium(IV) species to provide the product (Figure 2). The use of $PhI(OAc)_2$ to access high-valent palladium is well precedented, with the palladium(IV) species undergoing facile reductive elimination.[2(c),31]

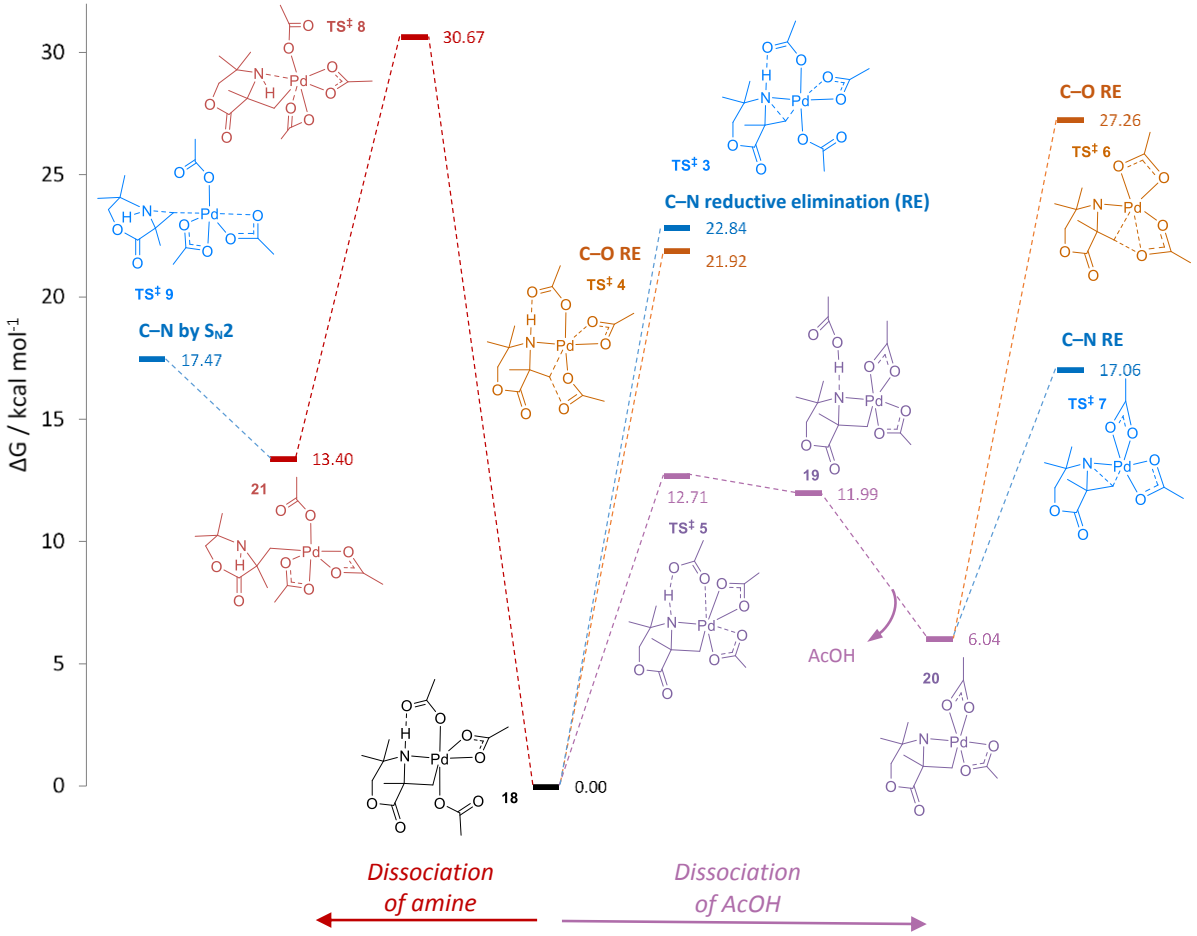

Figure 12. Possible pathways to form either a C–O or C–N bond. Reductive elimination from the initial palladium(IV) intermediate **18** is a high energy pathway and the reaction instead proceeds through rapid deprotonation of the coordinated amine, liberating acetic acid, to give intermediate **20**. Reductive elimination from this species is the lowest energy pathway and favors C–N bond formation (**TS‡ 7**). Even though the transition state for C–N bond formation through S_N2-type attack of the free amine, **TS‡ 9**, is similar in energy to the reductive elimination through **TS‡ 7**, accessing the necessary conformation is prohibitive due to the high energy barrier (*via* **TS‡ 8**) associated with the dissociation of the nitrogen atom from the metal center.

However, although reductive elimination from palladium(IV) is well known, the chemoselectivity of C–heteroatom reductive elimination is poorly understood where multiple competing pathways exist[32] and therefore any extra insight into this process is of high value. Reaction *via* a bimetallic palladium(III) intermediate as characterized by Ritter[33] was considered. However, this was deemed to be unlikely here due to the high energy species formed from the hindered amines stacking on top of each other in the palladium(III) dimer. This supposition was borne out by calculations which suggested that the palladium(IV) intermediate was more favorable.[34]

We initially tested the C–N and C–O reductive elimination pathways directly from the proposed palladium(IV) intermediate **18** (Figure 12).[35] Counter to our expectations, C–O bond formation *via* **TS‡ 4** was a lower energy process than C–N bond formation *via* **TS‡ 3**.[36] This reaction pathway is therefore not feasible because the resulting acetoxylated product (**16**) has been experimentally ruled out as an intermediate in the formation of the aziridine (Figure 8). We then considered the possibility of acetic acid dissociation from **18**, *via* **TS‡ 5**, to give complex **20** where the nitrogen atom now formally acts as an anionic ligand. Pleasingly, the C–N reductive elimination *via* **TS‡ 7** to form the aziridine was now lower in energy than both the competing C–O reductive elimination *via* **TS‡ 6** as well as the C–O reductive elimination *via* **TS‡ 4**. This is consistent with previous work on C–H amination with amide directing groups;[37] the nitrogen atoms are formally deprotonated in the proposed catalytic cycles and lead to C–N reductive elimination as the major pathway. The possible dissociation of acetic acid from the palladium(IV) intermediate is perhaps not too surprising as the electronegative oxygen atoms in the morpholinone may lead to an increase in acidity of the N–H bond and therefore lower the energy of the deprotonated pathway.

For completeness, we also calculated the pathway for C–N bond formation by S_N2-type attack by the uncoordinated amine. We found that even though the transition state of the C–N bond forming step, **TS‡ 9**, was comparable in energy with the lowest energy C–N reductive elimination transition state, **TS‡ 7**, the reactive conformation cannot be reached. In order for the geometry of the palladium(IV) species to be reactive to S_N2, the amine must

dissociate from the palladium(IV) center (breaking both the amine-palladium bond and the O–H hydrogen bond) and rotate. It was found that the energy required to do this was prohibitively high (**TS**‡ **8**) and so we do not believe that the S_N2 pathway is operable.

As a result of our studies we are now able to propose a more complete mechanistic picture of this unusual C–H activation reaction (Scheme 4). The amine **1** first coordinates to palladium acetate to give *mono*-coordinated intermediate **10**. This species can either coordinate to another amine, to form the off-cycle *bis*-amine intermediate **4**, or can undergo the TOLS of intramolecular C–H activation to form a four-membered ring palladacycle **11**. This intermediate is now susceptible to oxidation by $PhI(OAc)_2$ and forms palladium(IV) intermediate **18**. Dissociation of acetic acid precedes C–N reductive elimination to provide the aziridine product and also reforms the active catalyst. Furthermore, the overall concentration of amine **1** is modulated by an acid-mediated equilibrium which provides a slow release mechanism for the substrate into the cycle and limits formation of the off-cycle *bis*-amine intermediate **4**.

Scheme 4. Final catalytic cycle

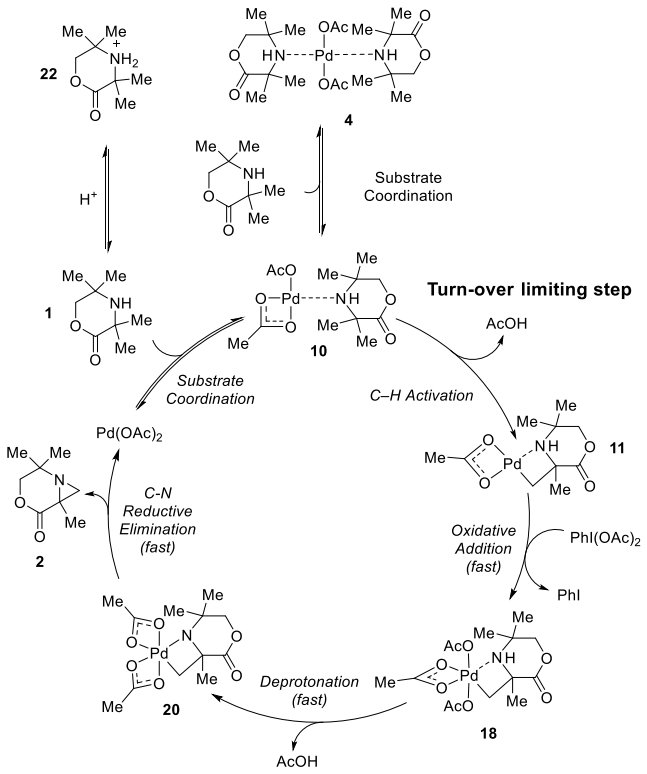

Conclusions

In summary, the mechanism of this novel native amine directed sp^3 C–H activation has been elucidated by detailed kinetic studies. Suppression of the formation of the off-cycle *bis*-amine complex by the addition of acetic acid was found to significantly increase the overall rate of reaction. The results of these studies have been used to improve yields of reaction, as well as providing a more synthetically useful procedure that is more applicable for large-scale chemistry. DFT calculations have given an insight into the regioselectivity of cyclopalladation and have provided a plausible explanation for the resulting aziridine product.

We are currently investigating how we can use this understanding to design ligands which can control the C–H activation step with the overall goal of creating an asymmetric process. We hope that these insights into the behavior of palladium(IV) leads to the rational design of related C–H functionalization reactions.

ASSOCIATED CONTENT

Supporting Information.
Experimental procedures, characterization data and computational details. This material is available free of charge via the Internet at http://pubs.acs.org.

AUTHOR INFORMATION

Corresponding Author

mjg32@cam.ac.uk

Notes

The authors declare no competing financial interest.

ACKNOWLEDGMENTS

We are grateful to the EPSRC and Pfizer (A.P.S.) for a studentship and the ERC and EPSRC for fellowships (M.J.G.). We are also grateful to Dr Alex Thom and Dr David Pryde (Pfizer) for helpful discussions. The computational work was performed using the Darwin Supercomputer of the University of Cambridge High Performance Computing Service (http://www.hpc.cam.ac.uk/), provided by Dell Inc. using Strategic Research Infrastructure Funding from the Higher Education Funding Council for England and funding from the Science and Technology Facilities Council. Mass spectrometry data were acquired at the EPSRC UK National Mass Spectrometry Facility at Swansea University.

REFERENCES

(1) (a) Jia, C.; Kitamura, T.; Fujiwara, Y. *Acc. Chem. Res.* 2001, 34, 633. (b) Godula, K.; Sames, D. *Science* **2006**, 312, 67. (c) Davies, H. M. L.; Manning, J. R. *Nature* **2008**, 451, 417. (d) Davies, H. M. L.; Du Bois, J.; Yu, J.-Q. *Chem. Soc. Rev.* **2011**, 40, 1855. (e) Yamaguchi, J.; Yamaguchi, A. D.; Itami, K. *Angew. Chem. Int. Ed.* **2012**, 51, 8960. (f) Mkhalid, I. A. I.; Barnard, J. H.; Marder, T. B.; Murphy, J. M.; Hartwig, J. F. *Chem. Rev.* **2010**, 110, 890.

(2) (a) Dupont, J.; Consorti, C. S.; Spencer, *J. Chem. Rev.* **2005**, 105, 2527. (b) Shilov, A. E.; Shul'pin, G. B. *Chem. Rev.* **1997**, 97, 2879. (c) Neufeldt, S. R.; Sanford, M. S. *Accounts Chem. Res.* **2012**, 45, 936.

(3) (a) Desai, L. V; Hull, K. L.; Sanford, M. S. *J. Am. Chem. Soc.* **2004**, 126, 9542. (b) Zaitsev, V. G.; Shabashov, D.; Daugulis, O. *J. Am. Chem. Soc.* **2005**, 127, 13154. (c) Giri, R.; Chen, X.; Yu, J.-Q. *Angew. Chem. Int. Ed.* **2005**, 44, 2112. (d) Campeau, L.-C.; Schipper, D. J.; Fagnou, K. *J. Am. Chem. Soc.* **2008**, 130, 3266. (e) Wang, D.-H.; Wasa, M.; Giri, R.; Yu, J.-Q. *J. Am. Chem. Soc.* **2008**, 130, 7190.

(4) (a) Giri, R.; Maugel, N.; Li, J.-J.; Wang, D.-H.; Breazzano, S. P.; Saunders, L. B.; Yu, J.-Q. *J. Am. Chem. Soc.* **2007**, 129, 3510. (b) Simmons, E. M.; Hartwig, J. F. *Nature* **2012**, 483, 70.

(5) Ryabov, A. D.; Sakodinskaya, I. K.; Yatsimirsky, A. K. *J. Chem. Soc. Dalt. Trans.* **1985**, 2629.

(6) McNally, A.; Haffemayer, B.; Collins, B. S. L.; Gaunt, M. J. *Nature* **2014**, 510, 129.

(7) Giri, R.; Liang, J.; Lei, J.-G.; Li, J.-J.; Wang, D.-H.; Chen, X.; Naggar, I. C.; Guo, C.; Foxman, B. M.; Yu, J.-Q. *Angew. Chem. Int. Ed.* **2005**, 44, 7420.

(8) Ferretti, A. C.; Brennan, C.; Blackmond, D. G. *Inorganica Chim. Acta* **2011**, 369, 292.

(9) (a) Blackmond, D. G. *Angew. Chem. Int. Ed.* **2005**, 44, 4302. (b) Baxter, R. D.; Sale, D.; Engle, K. M.; Yu, J.-Q.; Blackmond, D. G. *J. Am. Chem. Soc.* **2012**, 134, 4600.

(10) Jones, W. D.; Feher, F. *J. Acc. Chem. Res.* **1989**, 22, 91.

(11) Simmons, E. M.; Hartwig, J. F. *Angew. Chem. Int. Ed.* **2012**, 51, 3066.

(12) (a) Ryabov, A. D. *Chem. Rev.* **1990**, 90, 403. (b) Davies, D. L.; Donald, S. M. A.; Macgregor, S. A. *J. Am. Chem. Soc.* **2005**, 127, 13754.

(13) (a) Cai, G.; Fu, Y.; Li, Y.; Wan, X.; Shi, Z. *J. Am. Chem. Soc.* **2007**, 129, 7666. (b) Albrecht, M. *Chem. Rev.* **2010**, 110, 576.

(14) Hein, J. E.; Armstrong, A.; Blackmond, D. G. *Org. Lett.* **2011**, 13, 4300.

(15) Stephenson, T. A.; Morehouse, S. M.; Powell, A. R.; Heffer, J. P.; Wilkinson, G. *J. Chem. Soc.* **1964**, 3632.

(16) Postulated Fujiwara-type intermediate:

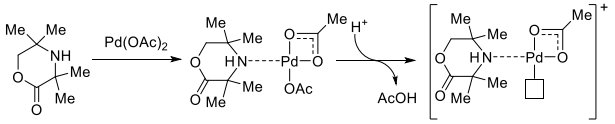

(17) Lu, W.; Jia, C.; Kitamura, T.; Fujiwara, Y. *Org. Lett.* **2000**, 2, 2927.

(18) (a) Nakata, K.; Yamaoka, Y.; Miyata, T.; Taniguchi, Y.; Takaki, K.; Fujiwara, Y. *J. Organomet. Chem.* **1994**, 473, 329. (b) Fujiwara, Y.; Takaki, K.; Watanabe, J.; Uchida, Y.; Taniguchi, H. *Chem. Lett.* **1989**, 1687.

(19) Explicit attempts to show that the main role of acetic anhydride was to dry the reaction were unsuccessful as addition of molecular sieves led to some decomposition of the starting material and $MgSO_4$ shut down the reaction.

(20) Addition of 1 equiv H_2O was found to shut down the reaction, providing < 5% product (see Supporting Information).

(21) Kerton, F. M.; Marriott, R. *Alternative Solvents for Green Chemistry;* Royal Society of Chemistry, **2013**, pp 14-15.

(22) Boutadla, Y.; Davies, D. L.; Macgregor, S. A.; Poblador-Bahamonde, A. I. *Dalton Trans.* **2009**, 5820.

(23) (a) Te Velde, G.; Bickelhaupt, F. M.; Baerends, E. J.; Fonseca Guerra, C.; van Gisbergen, S. J. A.; Snijders, J. G.; Ziegler, T. *J. Comput. Chem.* **2001**, 22, 931. (b) Fonseca Guerra, C.; Snijders, J. G.; te Velde, G.; Baerends, E. J. *Theor. Chem. Accounts Theory, Comput. Model. (Theoretica Chim. Acta)* **1998**, 99, 391. (c) ADF2014, SCM, Theoretical Chemistry, Vrije Universiteit, Amsterdam, The Netherlands, http://www.scm.com.

(24) (a) Wassenaar, J.; Jansen, E.; van Zeist, W.-J.; Bickelhaupt, F. M.; Siegler, M. A.; Spek, A. L.; Reek, J. N. H. *Nat. Chem.* **2010**, 2, 417. (b) Wolters, L. P.; van Zeist, W.-J.; Bickelhaupt, F. M. *Chemistry* **2014**, 20, 11370.

(25) Lyngvi, E.; Sanhueza, I. A.; Schoenebeck, F. *Organometallics* **2015**, 34, 805.

(26) Species **4** is slightly higher in energy than the conformer formed through ring flip which places the palladium pseudo equatorial. However, the subsequent transition states for C–H cleavage were found to be substantially higher in energy (see Supporting Information). Presumably, although the steric clash of the methyl groups of **4** results in a higher energy conformer, the resulting cyclopalladation is more favorable as a result of the C–H bonds being placed proximal to the metal center.

(27) Melander, L. C. S.; Saunders, W. H.; *Reaction Rates of Isotopic Molecules*; Wiley, **1980**, pp 44-45.

(28) (a) Rousseaux, S.; Gorelsky, S. I.; Chung, B. K. W.; Fagnou, K. *J. Am. Chem. Soc.* **2010**, 132, 10692. (b) García-Cuadrado, D.; Braga, A. A. C.; Maseras, F.; Echavarren, A. M. *J. Am. Chem. Soc.* **2006**, 128, 1066. (c) Balcells, D.; Clot, E.; Eisenstein, O. *Chem. Rev.* **2010**, 110, 749.

(29) (a) Gorelsky, S. I.; Lapointe, D.; Fagnou, K. *J. Org. Chem.* **2012**, 77, 658. (b) Usharani, D.; Lacy, D. C.; Borovik, A. S.; Shaik, S. *J. Am. Chem. Soc.* **2013**, 135, 17090. (c) De Jong, G. T.; Bickelhaupt, F. M. *Chemphyschem* **2007**, 8, 1170. (d) Ess, D. H.; Houk, K. N. *J. Am. Chem. Soc.* **2008**, 130, 10187. (e) Green, A. G.; Liu, P.; Merlic, C. A.; Houk, K. N. *J. Am. Chem. Soc.* **2014**, 136, 4575.

(30) Zhang, Q.; Yu, H.; Fu, Y. *Organometallics* **2013**, 32, 4165.

(31) (a) Hickman, A. J.; Sanford, M. S. *Nature* **2012**, 484, 177. (b) Sehnal, P.; Taylor, R. J. K.; Fairlamb, I. J. S. *Chem. Rev.* **2010**, 110, 824. (c) Dick, A. R.; Hull, K. L.; Sanford, M. S. *J. Am. Chem. Soc.* **2004**, 126, 2300. (d) Yoneyama, T.; Crabtree, R. H. *J. Mol. Catal. A Chem.* **1996**, 108, 35. (e) Muñiz, K. *Angew. Chem. Int. Ed.* **2009**, 48, 9412. (f) Cheng, X.-F.; Li, Y.; Su, Y.-M.; Yin, F.; Wang, J.-Y.; Sheng, J.; Vora, H. U.; Wang, X.-S.; Yu, J.-Q. *J. Am. Chem. Soc.* **2013**, 135, 1236.

(32) Camasso, N. M.; Pérez-Temprano, M. H.; Sanford, M. S. *J. Am. Chem. Soc.* **2014**, 136, 12771.

(33) Powers, D. C.; Ritter, T. *Nat. Chem.* **2009**, 1, 302.

(34) Possible palladium(III) bimetallic intermediate:

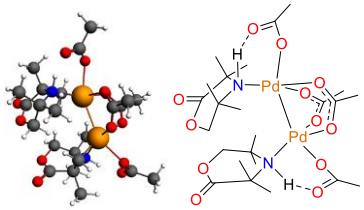

Pd(II) (**10**) + Pd(IV) (**11**) → Pd(III); ΔG = +8.4 kcal mol^{-1}

(35) Intermediate **18** is -39.7 kcal mol^{-1} lower in energy than intermediate **10**. Therefore, all species in Figure 12 are not kinetically relevant as expected from the experimental data.

(36) Changing the position of the acetate ligands on the palladium(IV) species gave higher energy intermediates (see Supporting Information). Also, note that the bidentate acetate trans to the substrate does not stop the C–N reductive elimination (to give **TS‡ 3**) from being symmetry allowed[38] as during the reaction the acetate binding changes from a κ^2 to a κ^1 coordination mode.

(37) (a) Nadres, E. T.; Daugulis, O. *J. Am. Chem. Soc.* **2012**, 134, 7. (b) He, G.; Zhao, Y.; Zhang, S.; Lu, C.; Chen, G. *J. Am. Chem. Soc.* **2012**, 134, 3. (c) Wang, C.; Chen, C.; Zhang, J.; Han, J.; Wang, Q.; Guo, K.; Liu, P.; Guan, M.; Yao, Y.; Zhao, Y. *Angew. Chemie Int. Ed.* **2014**, 53, 9884.

(38) Braterman, S. *J. Chem. Soc. Chem. Commun.* **1979**, 70.

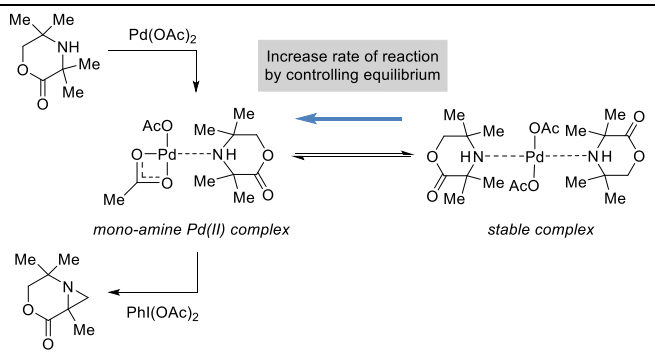

Insert Table of Contents artwork here